Ab initio study on surface segregation of hydrogen from diamond C(100) surfaces

C. Kanai,[1] Y. Shichibu,[1] K. Watanabe,[1,2] and Y. Takakuwa[3]
[1]*Department of Physics, Tokyo University of Science, 1-3 Kagurazaka, Shinjuku-ku, Tokyo 162-8601, Japan*
[2]*Frontier Research Center for Computational Sciences, Tokyo University of Science, 1-3 Kagurazaka, Shinjuku-ku, Tokyo 162-8601, Japan*
[3]*Institute of Multidisciplinary Research for Advanced Materials, Tohoku University, 2-1-1 Katahira, Aoba-ku, Sendai 980-8577, Japan*
(Received 12 October 2001; published 3 April 2002)

The segregation of a hydrogen (H) atom to the monohydride diamond C(100)2×1 surface from the subsurface, which consists of two elementary processes of lateral migration in the subsurface and migration to the surface from the bulk, has been investigated by *ab initio* pseudopotential method. Since the activation energy barrier (AEB) for H migration in the subsurface perpendicular to dimer rows markedly decreases due to the presence of an H defect on the surface, it becomes an easy diffusion path and the diffusing H atoms tend to approach a position under a hollow site. The AEB for H migration to the surface from the bulk also markedly decreases due to the H defect on the surface. Thus, the H defect on the monohydride surface is easily repaired by H atoms from the subsurface, resulting in the suppression of methane adsorption and diamond epitaxial growth. The theoretical results support the experimental observations.

DOI: 10.1103/PhysRevB.65.153312 PACS number(s): 71.15.−m, 81.05.Uw, 61.72.Ji

Due to recent technological advances in epitaxial diamond growth, obtaining diamond films is not difficult by means of the chemical vapor deposition (CVD) method,[1,2] but it is still very challenging to obtain single-crystalline diamond films with large surface areas. In diamond epitaxy, the behavior of hydrogen on the diamond surface influences the growth rate and the quality of diamond films. Thus, it is important to elucidate the chemical processes of hydrogen at the atomic level in order to understand the complicated mechanism of diamond growth. Many experiments[3–7] and theoretical[8–12] studies have been performed on hydrogen on diamond surfaces. Focusing on the role of hydrogen in diamond epitaxy, we have investigated the stability of hydrogenated diamond surfaces,[13] hydrogen desorption pathways under atomic hydrogen irradiation[14] and hydrogen etching of the graphite phase on the diamond surface[15] by using *ab initio* pseudopotential calculations.

Secondary-ion mass spectroscopy[16] and elastic recoil detection analysis[17] suggest that much hydrogen exists in the diamond subsurfaces. One of the reasons for the incorporation of hydrogen in the diamond subsurface is that hydrocarbons diluted with hydrogen as raw material gas are generally used in epitaxial diamond growth.[18] Therefore, hydrogen in the subsurface is predicted to influence diamond growth as well as hydrogen on the surface. By an analysis of the time evolution of surface hydrogen coverage, Nishimori *et al.*[7] demonstrated that the rate of surface hydrogen segregation from the bulk, leading to the suppression of diamond growth caused by hydrogen in the subsurface, is comparable to the rate of hydrogen desorption. They concluded that surface hydrogen has to be removed by means of a nonthermal method to increase the growth rate of diamond. Therefore, the effect of surface hydrogen segregation from the bulk has to be taken into account to reveal the complicated processes in diamond growth. Moreover, hydrogen in the diamond subsurface is also predicted to influence the surface electronic properties. For example, hydrogen in the subsurface might be the cause of the *p*-type conductive layer in CVD diamond films. Hayashi and co-workers[16,19] suggested that the surface conductivity of hydrogenated diamond surfaces depends on hydrogen incorporated in the subsurface region. Thus, it is important to theoretically investigate the energetics of hydrogen in the diamond subsurfaces and its effect on the surface electronic states for electronic device applications. Although many theoretical studies[20–23] on hydrogen in bulk diamond have been performed, to our knowledge, there have been no theoretical studies on hydrogen in the diamond subsurface. Therefore, the objectives of this study are to obtain the energetics and migration pathways of hydrogen atoms in the subsurface, and to predict the effect of hydrogen in the subsurface on epitaxial diamond growth using *ab initio* calculations.

In the present study, we performed self-consistent total-energy calculations within the framework of density-functional theory using the norm-conserving pseudopotential scheme.[24–26] The generalized gradient approximation by Perdew *et al.*[27] was used for the exchange-correlation potential. We employed the norm-conserving pseudopotentials obtained by Kobayashi[28] using the scheme of Troullier and Martins[29] for both carbon and hydrogen. The electron wave functions were expanded in a plane-wave basis set including plane waves up to a cutoff energy of 49 Ry. We chose 16 $\boldsymbol{k}$ points for the system of the diamond surface in the first Brillouin zone. In our calculations of the monohydride diamond surface, the substrate was modeled by a repeated slab for diamond C(100), which had eight atomic layers with c(4×4) atoms per layer and was separated by a vacuum region equivalent to twelve atomic layers. The dangling bonds on the bottom surface of the slab were saturated with hydrogen atoms. Atoms on the top six layers of the slab were relaxed, and those in the remaining two layers were fixed at their bulk positions.

Initially, we describe the most stable site for a hydrogen atom in the subsurface region under a monohydride C(100) surface. We calculated the total energies of the systems when a hydrogen atom is at three sites, i.e., bond center (BC) site,

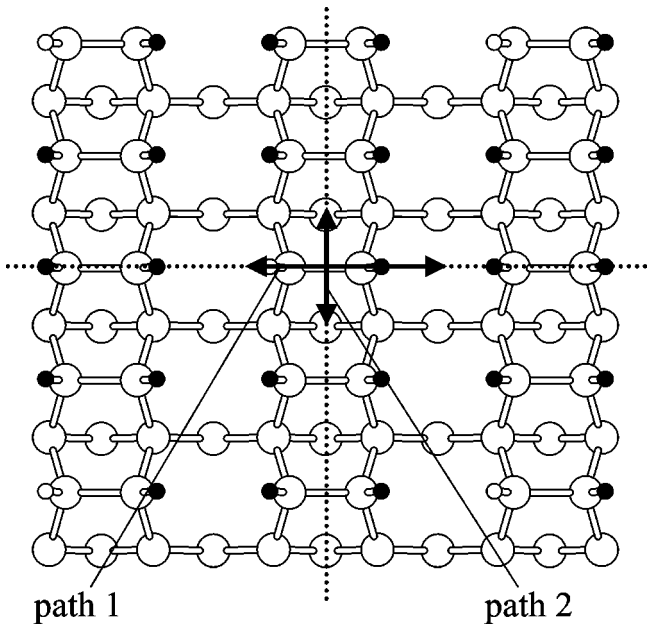

FIG. 1. Top view of monohydride C(100)2×1 surface. Open circles, small open circles and closed circles denote carbon atoms, hydrogen vacancies, and adsorbed hydrogen atoms, respectively. Path 1 and path 2 indicate the diffusion paths in the subsurface perpendicular to dimer rows and along dimer rows, respectively.

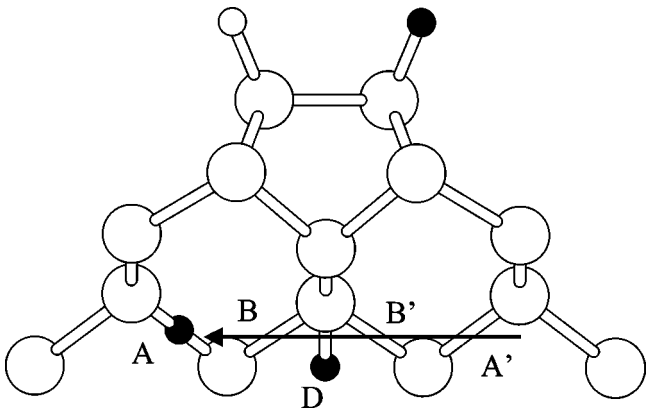

FIG. 2. Side view of monohydride C(100)2×1 surface. Path 1 in Fig. 1 is shown by an arrow. The definitions of the circles are the same as those in Fig. 1. *A*, *A′*, *B*, *B′* are bond center (BC) sites. *D* corresponds to a transition state between the two local minimum *B* and *B′*.

tetrahedral interstitial (*T*) site, and equilateral triangle (ET) site in the region of five to six atomic layers below the surface. The BC site is found to be the most stable one because the ET site and the *T* site are higher in energy by 1.09 eV and 1.23 eV than the BC site, respectively. Thus, some typical migration paths from one BC site to another BC site via a transition state have been chosen in this study. Regarding the most stable site in the bulk, our calculation gives also the BC site although Saada *et al.*[20] obtained the ET site that has slightly lower energy than the BC site by the tight-binding calculations. We do not focus on the difference between them further, because the difference is probably ascribed to the different numerical approaches and does not affect the main results in this study.

We investigated the effect of H defect (vacancy) of the monohydride C(100) surface [Fig. 1, a top view of monohydride C(100) surface] on H segregation from the bulk. Open circles small closed circles, and small open circles in Fig. 1 refer to carbon atoms, hydrogen atoms adsorbed on the carbon dimer atoms and hydrogen defects (five vacancies), respectively.

First, we describe the potential-energy curves (PEC's) for the lateral migration in the subsurface in two directions, perpendicular to the dimer rows (path 1 in Fig. 1) and along the dimer rows (path 2 in Fig. 1). Path 1 is represented by an arrow in a side view of the monohydride C(100) surface in Fig. 2. Position *D* is a transition state immediately below a dimer row and positions *A* and *A′* are stable BC sites under hollow sites.

In Fig. 3(a), the PEC's along path 1 are given when the surface is a perfect monohydride (solid line) and when it has H defects (broken line). The PEC for the perfect monohydride surface has two local minima (*B* and *B′*) under the dimer row, in addition to the lowest ones at *A* and *A′*. Activation energy barriers (AEB's) for migration from *B* to *B′* via transition state *D* and that from *A* to *B* are 0.64 eV and 1.34 eV, respectively. All of the positions *A*, *A′*, *B*, and *B′* are BC sites. In bulk diamond, these BC sites are equivalent and the AEB between them is 2.14 eV from our calculation under periodic boundary conditions without surface. Therefore, it is important to note that the (reconstructed) surface effect markedly influences the migration in the subsurface. It is also noted that a semiempirical cluster calculation by Mehandru *et al.*[22] gave an AEB of 1.9 eV for migration from one BC site to another BC site. The difference of 0.24 eV is considered to come mainly from the finite- size effect by the cluster calculations in addition to the semiempirical calculation.

When an H defect is generated on the surface (a small open circle in Fig. 2), the PEC is significantly changed with the disappearance of the local minima of *B* and *B′*, as shown by the broken line in Fig. 3(a). This indicates that the migrating H atom in the direction perpendicular to dimer rows in the subsurface is pulled toward position *A* by the H defect on the surface. On the other hand, the AEB for migration along the dimer row (path 2) is changed by only 10% due to the H defect, by comparing the two curves for perfect monohydride surface (solid line) and H-defect surface in Fig. 3(b), although a local maximum immediately below the dimer becomes a local minimum *M* when an H defect is introduced on the surface. However, position *M* is almost an unstable saddle point because position *M*, which is midway between positions *B* and *B′*, has high potential energy along path 1, as shown in Fig. 3(a). Thus, the results in Figs. 3(a) and 3(b) enable us to conclude that migrating H atoms in the subsurface tend to approach position *A* immediately below the H defect on the surface.

Next, we investigated H migration from the subsurface to the surface in the direction perpendicular to the surface. Two migration pathways chosen in this calculation are schematically shown by arrows in Fig. 4. The PEC's along path 3 are

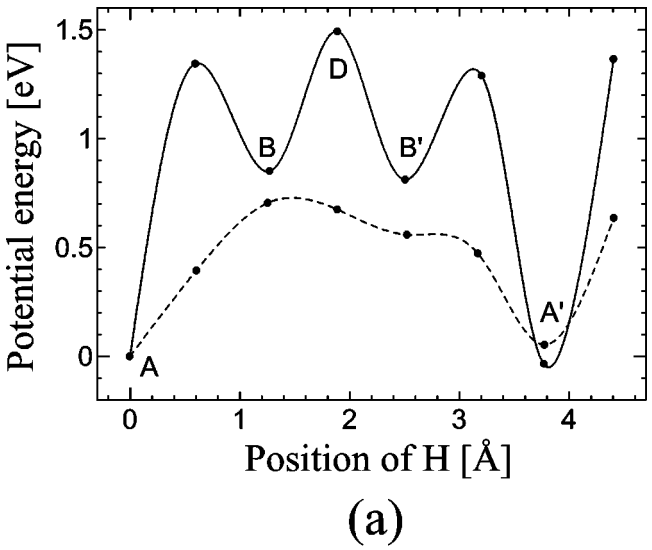

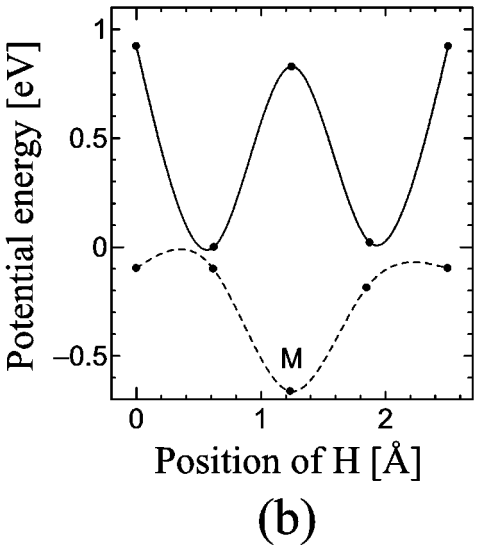

FIG. 3. Potential-energy curves for diffusion of a hydrogen atom in the subsurface along (a) path 1 and (b) path 2. Solid curves and broken curves are for the migration under the perfect monohydride surface and under the H defect monohydride surface, respectively. *A*, *B*, *D*, *B′*, *A′* are the H positions defined in Fig. 2.

given by a solid curve for the perfect monohydride surface and by a dashed curve for the H-defect surface in Fig. 5. The horizontal coordinate is the position of a migrating H atom measured from the stable position at the surface. The configurations corresponding to the right ends of the curves are such that the carbon atom with number 1 in Fig. 4 is a dihydride for a perfect monohydride surface (solid curve) and a monohydride for an H-defect surface (broken curve). Surprisingly, the AEB for the migration from the bulk to the surface almost disappears in the presence of a single H vacancy on the surface. It is obvious from these two curves that H migration toward the surface is significantly promoted by the H defect on the surface and as a result, an H vacancy tends to be repaired by the H atom coming from the subsurface.

The PEC along path 4 is not shown in Fig. 5, because its

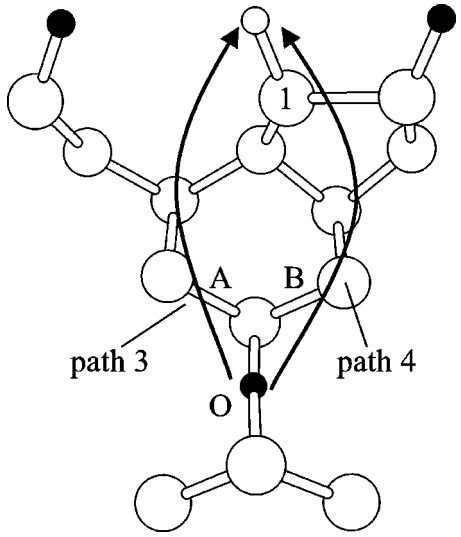

FIG. 4. Migration paths from subsurface to the surface in the side view of monohydride C(100)2×1 surface. Potential-energy curves are calculated for path 3 and path 4. The definitions of circles are the same as those in Fig. 1. *O*, *A*, and *B* are BC sites.

qualitative features are similar to those along path 3. The only difference between the two PEC's is that the AEB for migration along path 3 is slightly smaller than that for migration along path 4, because C-C bond stretching is more permissible for the former path than for the latter path when an H atom approaches a BC site, as clearly seen in the atomic geometry in Fig. 4. The present result on the PEC's in Fig. 5 provides a theoretical explanation for an experimental observation by Nishimori *et al.*[7] that methane adsorption and epitaxial diamond growth are suppressed by hydrogen atoms in the subsurface.

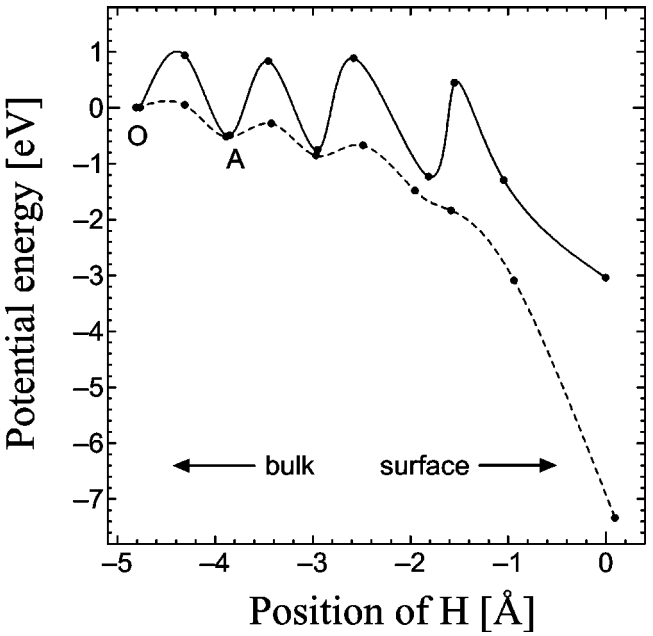

FIG. 5. Potential-energy curves for migration from subsurface to C(100) surface along path 3 defined in Fig. 4 when the surface is perfect monohydride (solid curve) and has hydrogen vacancy (broken curve).

In conclusion, we have calculated the PEC's for hydrogen segregation from the subsurface to the monohydride surface and found that a single hydrogen vacancy on the monohydride surface significantly changes the PEC's. The H vacancy on the surface makes the PEC for lateral migration perpendicular to dimer rows in the subsurface considerably smooth. As a result, migrating H in the subsurface tends to approach a position immediately under the H vacancy on the surface. Furthermore, H migration from the subsurface to the surface is considerably promoted by the H vacancy with an almost complete disappearance of the activation energy, resulting in a repair of the H vacancy by the H atom coming from the subsurface. The present results on H segregation from the subsurface provide a theoretical background for the experimental observation of the hydrogen effect on the growth rate of epitaxial diamond.

This work was supported by the JSPS Research for the Future Program in the Area of Atomic-Scale Surface and Interface Dynamics. C.K. thanks the Supercomputer Center, Institute for Solid State Physics, University of Tokyo for the use of their facilities.

[1] S. Matsumoto, Y. Sato, M. Kamo, and N. Setaka, Jpn. J. Appl. Phys., Part 2 **21**, L183 (1982).
[2] C.J. Chu, R.H. Huge, J.L. Margrave, and M.P. D'Evelyn, Appl. Phys. Lett. **61**, 1393 (1992).
[3] H. Kawarada, Surf. Sci. Rep. **26**, 205 (1996).
[4] H. Kawarada, H. Sasaki, and A. Sato, Phys. Rev. B **52**, 11 351 (1995).
[5] T. Nishimori, H. Sakamoto, Y. Takakuwa, and S. Kono, J. Vac. Sci. Technol. A **13**, 2781 (1995).
[6] T. Nishimori, H. Sakamoto, Y. Takakuwa, and S. Kono, Diamond Relat. Mater. **6**, 463 (1997).
[7] T. Nishimori, H. Sakamoto, Y. Takakuwa, and S. Kono, Diamond Films Technol. **6**, 301 (1996).
[8] J. Furthmüller, J. Hafner, and G. Kresse, Phys. Rev. B **53**, 7334 (1996).
[9] C.C. Battaile, D.J. Srolovitz, I.I. Oleinik, D.G. Pettifor, A.P. Sutton, S.J. Harris, and J.E. Butler, J. Chem. Phys. **111**, 4291 (1999).
[10] X.Y. Chang, M. Perry, J. Peploski, D. Thompson, and L.M. Raff, J. Chem. Phys. **99**, 4748 (1993).
[11] D. Huang and M. Frenklach, J. Phys. Chem. **96**, 1868 (1992).
[12] M. Frenklach and S. Skokov, J. Phys. Chem. B **101**, 3025 (1997).
[13] C. Kanai, K. Watanabe, and Y. Takakuwa, Jpn. J. Appl. Phys., Part 2 **38**, L783 (1999).
[14] C. Kanai, K. Watanabe, and Y. Takakuwa, Appl. Surf. Sci. **159-160**, 599 (2000).
[15] C. Kanai, K. Watanabe, and Y. Takakuwa, Phys. Rev. B **63**, 235311 (2001).
[16] K. Hayashi, S. Yamanaka, H. Okushi, and K. Kajimura, Appl. Phys. Lett. **68**, 376 (1996).
[17] H. Yagi, A. Hatta, and T. Ito, Appl. Surf. Sci. **137**, 50 (1999).
[18] T. Ando, M. Ishii, M. Kamo, and Y. Sato, J. Chem. Soc., Faraday Trans. **89**, 1783 (1993).
[19] K. Hayashi, S. Yamanaka, H. Watanabe, T. Sekiguchi, H. Okushi, and K. Kajimura, J. Appl. Phys. **81**, 744 (1997).
[20] D. Saada, J. Adler, and R. Kalish, Phys. Rev. B **61**, 10 711 (2000).
[21] S.K. Estreicher, M.A. Roberson, and D.M. Maric, Phys. Rev. B **50**, 17 018 (1994).
[22] S.P. Mehandru, A.B. Anderson, and J.C. Angus, J. Mater. Res. **7**, 689 (1992).
[23] P. Briddon, R. Jones, and G.M.S. Lister, J. Phys. C **21**, L1027 (1988).
[24] M.C. Payne, M.P. Teter, D.C. Allan, T.A. Arias, and J.D. Joannopoulos, Rev. Mod. Phys. **64**, 1045 (1992).
[25] P. Hohenberg and W. Kohn, Phys. Rev. **136**, B864 (1964).
[26] W. Kohn and L.J. Sham, Phys. Rev. **140**, A1133 (1965).
[27] J.P. Perdew, J.A. Chevary, S.H. Vosko, K.A. Jackson, M.R. Pederson, D.J. Singh, and C. Fiolhais, Phys. Rev. B **46**, 6671 (1992).
[28] K. Kobayashi, Comput. Mater. Sci. **14**, 72 (1999).
[29] N. Troullier and J.L. Martins, Phys. Rev. B **43**, 1993 (1991).